VCSEL Based Coherent PONs

Jesper Bevensee Jensen, Roberto Rodes, Antonio Caballero, Ning Cheng,
Darko Zibar, and Idelfonso Tafur Monroy

***Abstract*—We present a review of research performed in the area of coherent access technologies employing vertical cavity surface emitting lasers (VCSELs). Experimental demonstrations of optical transmission over a passive fiber link with coherent detection using VCSEL local oscillators and directly modulated VCSEL transmitters at bit rates up to 10 Gbps in the C-band as well as in the O-band are presented. The broad linewidth and frequency chirp associated with directly modulated VCSELs are utilized in an envelope detection receiver scheme which is demonstrated digitally (off-line) as well as analog (real-time). Additionally, it is shown that in the optical front-end of a coherent receiver for access networks, the 90° hybrid can be replaced by a 3-dB coupler. The achieved results show that VCSELs are attractive light source candidates for transmitter as well as local oscillator for coherent detection PONs**

***Index Terms*—Access networks, coherent detection, optical communication systems, passive optical networks (PONs), vertical cavity surface emitting lasers (VCSEL).**

I. Introduction

HIGHER capacity, more flexibility, wireless/wireline integration, *and* reduced cost and power consumption. These are some of the requirements we expect future optical access networks to cope with. For the European region, the EU has defined a strategy for information and communication technology (ICT)—the *digital agenda 2020*—which sets as a target that by 2020, download rates of 30 Mbps should be available to all EU citizens and 100 Mbps to 50% of the European households [1], and the forward looking international group of service providers *The Full Service Access Network (FSAN) Group* has a goal of 1 Gbps end user capacity capabilities for next generation passive optical networks (NG-PON2) [2].

Expecting to meet these requirements through a scaling of current time division multiplexed (TDM) direct detection PON technologies seems highly optimistic at best, and therefore other alternatives are at present being investigated by various research groups and companies. These alternatives include various flavours of wavelength division multiplexed (WDM) access, coherent detection access networks and the employment of low-cost vertical cavity surface emitting lasers (VCSELs).

This paper presents a review and elaboration of results achieved at DTU Fotonik within coherent optical access networks employing directly modulated VCSELs (DM-VCSEL). Parts of these results have previously been presented in [3]–[6], and they are presented here together with added details on the demodulation technique and with a more in-depth discussion of the issue of chirp and optical fiber chromatic dispersion (CD), and how the two interplay in the presented experiments. We present coherent detection transmission demonstrations employing VCSELs as both local oscillator (LO) and as DM transmitter light source in the O-band as well as in the C-band. Results employing off-line digital signal processing (DSP) as well as real-time analog signal processing are presented. As the background, we present examples from the history of coherent optical access networks and provide an overview of the current state of the art in this field.

Based on the results presented in this paper, coherent PONs employing VCSELs appear as a strong technology platform candidate capable of meeting these demands in a cost effective manner.

Section I gives a brief overview of the history and recent developments within coherent optical access networks, Section II introduces the coherent DM–VCSEL signalling method proposed in the paper, Section III collects results from experimental demonstrations, and Section IV gives a conclusion of the paper. The reader who is familiar with coherent detection in optical access networks can jump directly to Section II from here.

A. Next Generation Optical Access Networks

A reduction in cost and complexity of optical access can be brought about by a consolidation of optical line terminations (OLTs) and the resulting reduction in the number of central offices (COs). In order to achieve this goal, PON reach must be increased from the 10 or 20 km specified in GPON. As a data point, the number of COs in Germany could be reduced by almost a factor of 10 from 8000 to 900 if the PON reach was increased to 50 km [7]. In this way, the number of end users, or ONUs, served by each OLT can be increased. This, however, requires at the same time an increase in the reach and in the passive splitting ratio of the PON links. An increase from the typically 32 or 64 ONUs per OLT to as much as or above 1000 has been suggested by, e.g., the Open Lambda Initiative [8].

Traditional TDM–PON architechtures as employed in, e.g., EPON, GPON or 10G-EPON do not, however, support neither the required increase in splitting ratio nor the extended reach. In order to bridge this gap, alternative PON architectures employing WDM have been investigated heavily in recent years.

Manuscript received September 13, 2013; revised December 19, 2013 and January 24, 2014; accepted January 27, 2014. Date of publication February 10, 2014; date of current version March 9, 2014.

J. B. Jensen, A. Caballero, D. Zibar, and I. T. Monroy are with the DTU Fotonik, Department of Photonics Engineering, Technical University of Denmark, 2800 Kongens Lyngby, Denmark (e-mail: jebe@fotonik.dtu.dk; acaj@fotonik.dtu.dk; dazi@fotonik.dtu.dk; idtm@fotonik.dtu.dk).

R. Rodes is with the Finisar, Sunnyvale, CA 94089 USA (e-mail: roberto.rodes@finisar.com).

N. Cheng is with the HUAWEI, CA 95050, USA (e-mail: ning.cheng@huawei.com).

Color versions of one or more of the figures in this paper are available online at http://ieeexplore.ieee.org.

Digital Object Identifier 10.1109/JLT.2014.2305572

Several architectures and modulation schemes have been investigated, including downtransmission of seed-light from the CO to the ONU with subsequent remodulation by a reflective semiconductor optical amplifier, see e.g. [9]–[14]; and hybrid TDM–WDM PON architechtures [15]–[25]. Many of these examples employ wavelength division demultiplexing at the remote node or local exchange based on either arrayed waveguide gratings (AWG) or wavelength selective switches; both being solutions which add cost and complexity, and with regards to the AWG introduce a fixed wavelength routing scheme. Fixed wavelength filters in the transmission path between OLT and ONU is unattractive as it makes dynamic and efficient allocation of resources and capacity challenging. Additionally, it will increase the risk of propriety or operator specific wavelength allocation which can work against societal demands of a democratization of ICT access and infrastructure.

An alternative, and potentially considerably simpler approach is to introduce coherent detection, optionally in combination with DSP, in the access networks. The advantages of this is twofold: first, the receiver sensitivity, and thereby the reach and power budget is boosted by the power of the LO laser, and second, coherent detection opens the possibility of channel selection at the receiver side through LO tuning. Receiver side channel selection facilitates the elimination and avoidence of fixed optical filters such as AWGs. This increases greatly the compatibility with various modulation formats and signal bandwidths, and additionally enables reconfigurable bandwidth allocation as all channels in principle are available to all receivers.

B. Coherent Detection in Optical Access

The idea of employing coherent detection in the access network is by no means new. Before the widespread success of the erbium doped fiber amplifier (EDFA) in the late 1990's, extensive research was performed in order to explore the possibilities provided by coherent detection in optical access networks. As early as 1989, an experimental demonstration of coherent detection of six wavelength channels, frequency shift keying modulated at 200 Mbps, was reported [26]. Channel spacing was an impressively low 2.2 GHz, and channel selection was performed by wavelength tuning of the LO laser. In [27] four-level differential polarization shift keying was used in combination with coherent detection to achieve a bit rate of 150 Mbps. Wavelength selective optical packet switching employing coherent detection has been presented in 1990 [28]. In 1992, radio frequency (RF) subcarrier multiplexing is realized in a star network architecture where light from a single laser is distributed to all users [29]. The individual users are identified by their subcarrier frequency. The idea of employing LO tuning for channel selection in coherent WDM access networks was further investigated in the European research project RACE/COBRA. Alberquerque [30] describes an experimental demonstration and Bachus *et al.* [31] describes four field trials carried out towards the end of the project. In [32] a passive star architecture employing coherent detection for multichannel optical transmission is presented. Data rates up to 140 Mbps are reported, and packet loss is kept at a minimum through the use of a specially developed Ethernet protocol.

From the late 1990's to around 2005, due to a combination of the success of WDM optical networks employing EDFAs and demultiplexing in AWGs on one side and the challenges involved with coherent detection—receiver complexity and phase/frequency-locking of the LO laser—on the other, the research interest in coherent access systems faded.

In recent years, however, coherent access technologies have gained renewed interest. In 2006, a coherent PON employing amplitude shift keying modulation for downstream transmission and minimum shift keying modulation for upstream transmission was demonstrated. DSP at the receiver enabled a simplification of receiver-side hardware [33]. In 2009, a coherent optical access network employing a ring topology was proposed and demonstrated [34]. In 2010, a 44 Gbps upstream transmission bit rate was achieved through orthogonal frequency division multiplexing (OFDM) and OLT-side coherent detection [35]. In 2011, Nyquist shaped WDM channels were used for upstream transmission of polarization multiplexed quarternary phase shift keying (QPSK) at 100 Gbps over an 80 km PON link with OLT side coherent detection [36]; the use of OFDM in optical access with direct or coherent detection is discussed in [37] with the conclusion that complexity is an issue; in [8] coherent WDM PONs with ultra-dense channel spacing is advocated; and converged transport of wireline and wireless types of signals are enabled by coherent detection with reconfigurable DSP in [38] and [39]. In 2012, an ultra-dense WDM architecture featuring 2 Gbps QPSK modulated WDM channels spaced by only 6.5 GHz was presented [40]; an OFDM based TDM–WDM hybrid with up to 130 km reach was presented [41]; in [42], a comparative analysis of external cavity laser (ECL) based and distributed feedback (DFB) laser based 40 Gbps QPSK modulated coherent PON showed less than 1 dB penalty for the DFB case; and in [43], a simplified receiver structure for coherent PON is enabled by phase scrambling of the LO.

Coherent detection in optical access networks was included in the initial discussions for the standardization on NG-PON2 [44], and coherent PON was considered by the FSAN Group as one of the potential candidates for NG-PON2 [45]. In the published recommendation ITU-T G.989.1, however, coherent detection is no longer mentioned.

In many of the examples of a "second wave" of coherent optical access research cited previously, it can to a certain degree be argued that the low level of complexity needed for a solution for optical access networks to achieve widespread deployment and commercial success has been sacrificed in the quest for higher performance. Technological solutions such as AWGs, very advanced signal processing and ECLs have been "borrowed" from the core network and applied with great success in terms of performance, but with some disregard for the cost and complexity issues that characterize access networks. Nevertheless, these results clearly demonstrate the potential of coherent technologies in optical access networks.

By combining coherent optical access networks with DM-VCSELs, a potentially attractive solution emerges where the increased cost and complexity of the coherent receiver is

mitigated by the reduced cost and complexity of DM-VCSELs. Apart from the work gathered and presented in this paper, very little work has been done with respect to coherent detection using VCSELs. In 2010, an experimental demonstration of a VCSEL employed as LO for QPSK transmission with coherent detection was reported [46]. In this example, however, the transmitter was an externally modulated DFB laser. In 2013, a very impressive demonstration of 960 km transmission of a 105.7 Gbps polarization multiplexed three-level pulse amplitude modulated signal was reported [47]. Here, an ECL was used as LO, and the fiber link employed EDFAs.

In this paper, we review experimental demonstrations of up to 105 km fully passive transmission and coherent detection of DM-VCSELs at bit rates up to 10 Gbps. The reported results—in the C-band as well as in the O-band—show that VCSELs are attractive light source candidates for the transmitter as well as for the LO for coherent PONs. The frequency chirp associated with DM-VCSELs are utilized in an envelope detection receiver scheme which is demonstrated digitally (off-line) as well as analog (real-time).

II. Coherent Detection Using VCSELs

Optical coherent detection involves optical beating of the incoming signal with a well defined reference—a LO laser. The photodetector thus records an optical interference signal between the signal and the LO. Provided that the LO is a well known fixed reference, it is possible to recover not only the magnitude of the signal, but also the phase and frequency information. Neglecting dc terms, and assuming that the optical power of the LO is much higher than the optical power of the signal, from standard theory on optical coherent detection—see e.g. chapter 10 in [48]—we know that the photodiode output signal $I_{\mathrm{AC}}(t)$ can be written as

$$I_{\mathrm{AC}}(t) = 2R\sqrt{P_{\mathrm{S}}P_{\mathrm{LO}}}\cos(\omega_{\mathrm{IF}}t + \Delta\phi) \tag{1}$$

where R is the responsivity of the photodiode, P_{S} and P_{LO} is the optical power of the signal and LO respectively, ω_{IF} is the intermediate frequency defined as the frequency difference between the signal and the LO, and $\Delta\phi$ is the phase offset between signal and LO. From (1) we can observe the well known advantages and drawbacks of coherent detection:

1) The signal power is boosted by the LO
2) The information stored in the optical phase and frequency as well as on the power of the signal can be recovered
3) If the phase and frequency information of the signal is to be recovered, the phase and frequency offset between the signal and the LO must be known

Obviously, the latter is what prevented widespread deployment of coherent optical communication systems before the breakthrough of high speed DSP.

For core networks, the main attraction of coherent detection is the possibility of storing information in the phase and frequency as well as in the power of the optical signal, and the potential gain in spectral efficiency provided by this. For access networks, it is (for now) mainly the boost in receiver sensitivity. Combining this with DM-VCSELs makes for a very attractive solution for optical access networks.

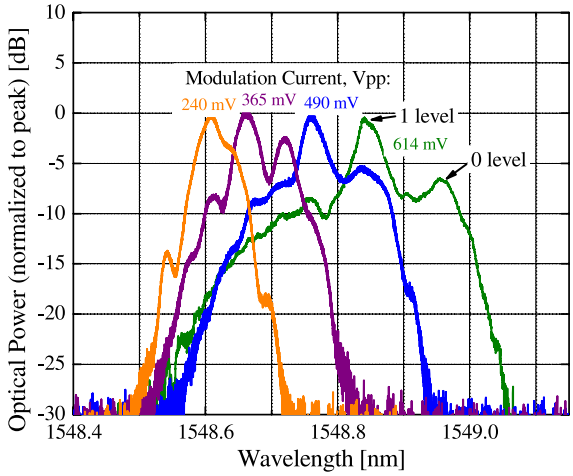

Fig. 1. Optical spectrum (normalized to peak power) of a 10 Gbit/s NRZ modulated VCSEL at different peak-to-peak modulation voltages. The spectra is measured with the 0.08 pm resolution Bosaphase optical spectrum analyzer. (See Figure from [52].)

A. Chirp-Assisted Envelope Detection

Traditionally, due to the apparent requirement of a stable phase and frequency relation between signal and LO, coherent detection has belonged to the realm of externally modulated low linewidth lasers far from the domain of the frequency chirped signals from DM-VCSELs. But it is exactly this chirp which enables us to employ the envelope detection based coherent detection of DM-VCSELs.

The frequency chirp $\Delta\nu$ associated with direct modulation of a VCSEL can be described as [49]–[51]:

$$\Delta\nu(t) = -\frac{\alpha}{4\pi}\left(\frac{d}{dt}\ln P(t) + \kappa P(t)\right) \tag{2}$$

where α is the linewidth enhancement factor defined as $\frac{\partial n'/\partial N}{\partial n''/\partial N}$, N being the carrier density and $n = n' + n''$ is the complex refractive index, $\ln P(t)$ is the logarithm of the instantaneous optical power, and κ is a structure dependent constant which is proportional to the modal confinement factor and inversely proportional to the volume of the active region, the optical frequency and the differential quantum efficiency.

The term $\frac{d}{dt}\ln P(t)$ in (2) describes the transient chirp which is proportional to the time derivative of the instantaneous optical power at the rising and falling edges of the pulse. The term $\kappa P(t)$ describes the adiabatic chirp related to the instantaneous optical power itself. We observe that as the transient chirp only effects the leading and trailing edges of the pulse, the optical wavelength of the high power 'one' state is lower than the optical wavelength of the 'zero' state. This is verified by Fig. 1 where the optical spectrum of the 1550-nm VCSEL used in the C-band experiments are plotted for constant bias and varying modulation depth. In all cases, the VCSEL is modulated by a 10 Gbps non-return-to-zero (NRZ) data signal from a pulse pattern generator. The spectra are measured with the

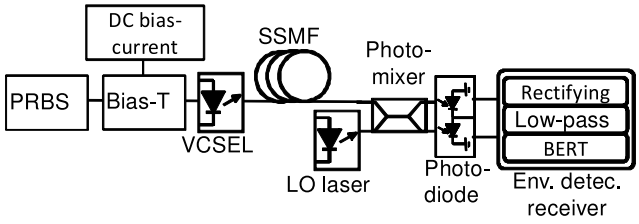

Fig. 2. Block diagram of the coherent VCSEL transmission system consisting of a pseudo-random binary sequence (PRBS) generator and a dc bias current source to directly modulate a VCSEL, standard singlemode fiber (SSMF), a local oscillator (LO) laser, a photomixer (can be either a 90° optical hybrid or a 3-dB coupler), a (balanced) photodiode, and the envelope detection receiver, which can be implemented analogue or digitally.

0.08 pm resolution Bosaphase optical spectrum analyzer. This fine resolution makes it possible to clearly identify the individual peaks corresponding to the 'zero' and 'one' states. The lower wavelength of the 'one' state is clearly visible. It can also be observed that the wavelength spacing between the two states increase with increasing modulation depth. The overall spectral shift to higher wavelengths with increasing modulation depth is caused by the increased temperature of the device due to higher root mean square value of the signal voltage at higher peak to peak voltage.

The clear wavelength separation between the 'zero' and 'one' states can be utilized in the coherent detection by tuning the LO laser wavelength close to the 'one' wavelength of the signal. This will convert the signal to a RF-like signal that can be demodulated by a simple envelope detection scheme consisting of squaring and low-pass filtering.

Although no frequency or phase locking between signal and LO is required, it is important that their frequency separation remains smaller than the bandwidth of the photodiode used in the receiver. In practice, this requires tuning of the LO wavelength. In the experiments with a VCSEL as LO described in this paper, this is achieved by tuning the bias current of the LO-VCSEL. The reported experiments are performed without temperature control or cooling. In a commercial implementation, temperature control is an option that can be considered and evaluated in terms of complexity versus performance.

The increased width of the VCSEL spectrum with increasing modulation depth imposes a lower boundary on the channel spacing in a WDM scenario in order to avoid optical interference between neighboring channels. In this case, 100 GHz channel spacing would be sufficient, but this will depend on the particular VCSEL used.

A functional block diagram of the setup used for the coherent detection of DM-VCSEL signals is shown in Fig. 2. A pseudo-random binary sequency (PRBS) of wordlength $2^{15}-1$ is combined with a dc bias current in a bias-T and used to directly modulate the VCSEL. The signal is propagated over a span of standard single mode fiber (SSMF). At the receiver, the signal is mixed with continuous wave light from a LO laser (ECL or VCSEL) in either a 3-dB coupler or a 90° optical hybrid coupler. The 3-dB coupler has the advantage of simplicity and requires half the number of photodiodes with respect to the 90° hybrid coupler, which on the other hand has the advantage

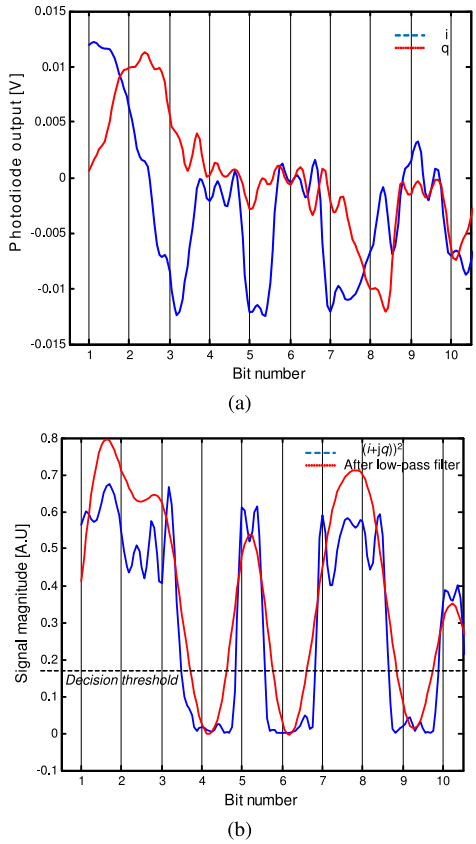

Fig. 3. Ten-bit section of the received signal at the individual steps of the envelope detector. (a) Shows the outputs (i and q) into a 50-Ω load directly after the photodiodes. (b) Shows the absolute value squared $(i+\mathrm{j}q)^2$ before (blue) and after (red) low-pass filtering.

of providing access to the in-phase as well as the quadrature component of the signal. This can be utilized for, e.g., digital dispersion compensation, which is an advantage in the C-band. The output from the coupler/hybrid is detected by photodiodes (balanced or single-ended), and demodulated by an envelope detector consisting of rectification, low pass filtering and bit error rate testing (BERT).

The signal at the different steps of the demodulation is shown in Fig. 3. The in-phase (i) and quadrature (q) output from the coherent detection is plotted in Fig. 3(a) for a signal of 10 bits duration with pattern [1 1 1 0 1 0 1 1 0 1]. The RF-like nature of the detected signal can be observed by the high positive or negative value in the one-bits and a value close to zero on the zero-bits. In Fig. 3(b), the magnitude of the combined i and q, i.e. $(i+\mathrm{j}q)^2$ is plotted with (blue) and without low-pass filtering (red). After low-pass filtering, the original NRZ data has been perfectly reconstructed with no use of digital or analogue phase locking of the signal and LO. The signal from the DM-VCSEL has thus been coherently detected employing a low complexity receiver algorithm based on envelope detection.

III. Experimental Demonstrations

Employing the method described previously, several experimental demonstrations were conducted with VCSELs operating

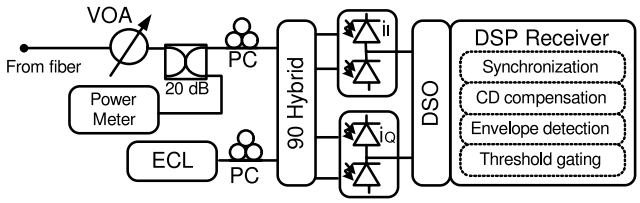

Fig. 4. Detail of the receiver implementation used for the 1550 nm experiments with ECL LO. A 90° optical hybrid is employed for the photomixing, and the signal after photodetection is stored by a digital storage oscilloscope (DSO) for off-line processing.

in the C-band around 1550 nm as well as with VCSELs operating in the O-band close to the 1300 nm zero-dispersion wavelength for SSMF. The experimental setups used in those demonstrations were variations over the scheme illustrated in Fig. 2. All experiments employed PRBS sequences with a word length of $2^{15}-1$. Adjustment of bias current and drive voltage for the VCSELs is performed by optimizing the extinction ratio while limiting amplitude overshoot. For both the C-band and the O-band VCSEL, this resulted in an extinction ratio of approximately 6.8 dB. The linewidth of both VCSELs are approximately 300 MHz, and their modulation capability is 10 Gbps. Since the envelope detection does not require any phase recovery, this broad linewidth is not critical for the coherent detection. The different experiments, and their results are described in the following.

A. C-Band Transmission With ECL LO

The experimental setup used in the demonstrations at 1550 nm wavelength is shown in Fig. 2 with details of the receiver implementation shown in Fig. 4. A tunable ECL serves as the LO, and the light from this is mixed with the incoming optical signal in a 90° optical hybrid coupler. After photodetection by two pairs of balanced photodetectors the signal is stored for off-line processing by a digital storage oscilloscope (DSO) with a sampling rate of 40 GSa/s. The off-line processing consists of synchronization, CD compensation, and envelope detection as described in Section II.

The CD compensation algorithm consists of fast Fourier transform of the received complex-valued signal, multiplication with the inverse transfer function $H^{-1}(f)$ of the dispersive fiber, and inverse fast Fourier transform to return to time-domain. The inverse transfer function of the dispersive fiber only takes first-order dispersion into account, and is given by (3).

$$H^{-1}(f) = e^{-j(d\cdot f)}, d = \pi \cdot d\frac{\lambda \cdot L}{\mathrm{c}} \tag{3}$$

where f is the optical center frequency, d is the first-order dispersion parameter (approximately 17 $\frac{\mathrm{ps}}{\mathrm{nm}\cdot\mathrm{km}}$ for SSMF), λ is the optical wavelengh, c is the speed of light in vacuum, and L is the length of the fiber.

The system was tested at 5 Gbps with optical transmission over 105 km SSMF and at 10 Gbps with 25 km SSMF transmission. Optical (direct detection) eye diagrams of the 5 and 10 Gbps back-to-back (B2B) signals are shown in Fig. 5. The VCSEL is biased at 13.6 mA and drive voltage is 1 V peak to peak.

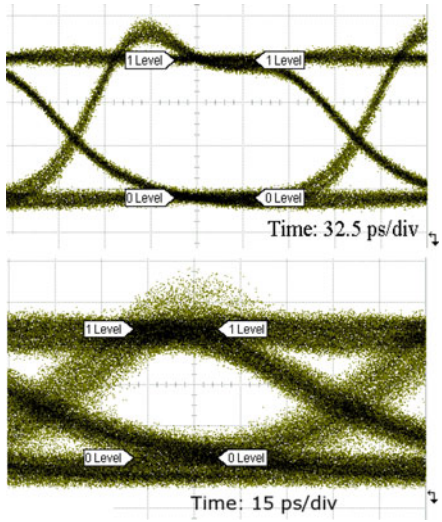

Fig. 5. Optical direct detection eye diagrams of the 5 Gbps and 10 Gbps back-to-back (B2B) signals from the 1550 nm VCSEL.

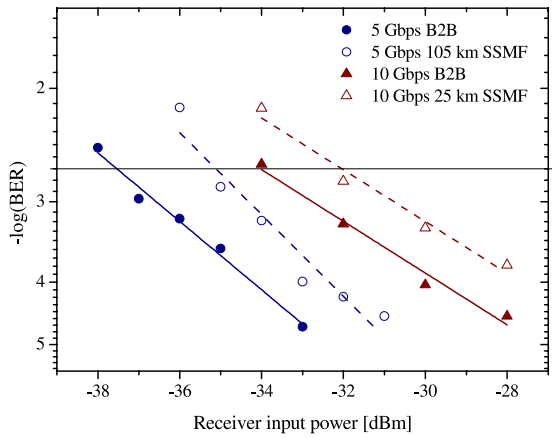

Fig. 6. BER of the 1550 nm signals at 5 Gbps and 10 Gbps B2B and after 105 km and 25 km SSMF transmission respectively.

Launch power into the fiber is approximately 1 dBm. Bit error ratio (BER) back to back (B2B) and after transmission is plotted in Fig. 6. At 5 Gbps, receiver sensitivity at the forward error correction (FEC) limit of 2×10^{-3} is -37.7 dBm and -35.1 dBm B2B and after 105 km transmission respectively, corresponding to a transmission power penalty of 2.6 dB. At 10 Gbps, the receiver sensitivity is -34.0 dBm B2B and -32.0 dBm after 25 km transmission, corresponding to a penalty of 2 dB. The penalty is mainly attributed to non-optimum polarization alignment between the signal and the LO. Numerical simulations in *VPI Transmission Maker* estimate the direct detection receiver sensitivity to be -22 dBm B2B at both 10 and 5 Gbps with a photodetector bandwidth of 7.5 GHz and no additional filtering in both cases. Alpha parameter (chirp), bias and peak to peak current of the drive signal is adjusted such that the optical spectrum and the extinction ratio match the experimental results. After 25 km transmission the simulated receiver sensitivity at 10 Gbps is -19 dBm. The 5 Gbps signal can not be recovered with direct detection after 105 km due to the combined effect of chirp and CD. For the 10 Gbps signal after 25 km SSMF,

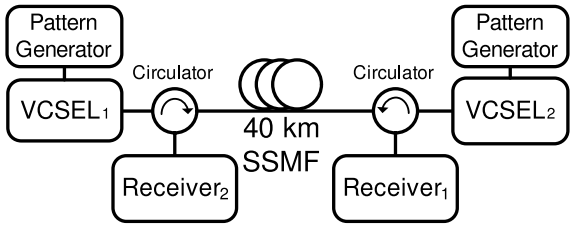

Fig. 7. Experimental setup of the bidirectional system. At each end, the signals transmitter and receiver signals are separated by optical circulators. Transmission is over 40 km SSMF, and the receivers are similar to Fig. 4.

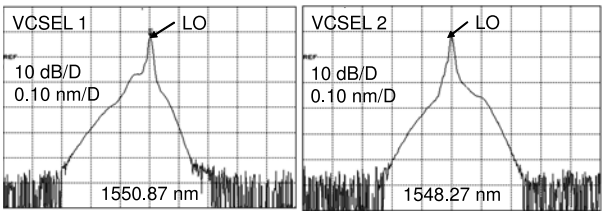

Fig. 8. Optical spectrum of the two signals in the bidirectional coherent VCSEL demonstration.

comparison between the simulated direct detection case and the experimentally demonstrated coherent detection indicates a possibility for at least 13 dB better performance for the coherent detection case.

1) Bidirectional C-Band Transmission: The 1550 nm 5 Gbps system has been demonstrated in a bidirectional configuration with 40 km SSMF transmission. The setup for the experiment is shown in Fig. 7. Two VCSELs are employed as the two transmitters, and an ECL is employed as LO laser. In each end, the signals to the receivers are separated from the signals from the transmitters by optical circulators. The optical spectra of the two signals are shown in Fig. 8. An advantage of the coherent detection in bidirectional systems employing the same wavelength band for upstream and downstream is that the beating between the Brillouin backscattered light and the LO will fall at a frequency outside the photodiode bandwidth due to the Brillouin shift of approximately 9.5 GHz. In our case, the two VCSELs are emitting at slightly different wavelengths in order to achieve identical output power and extinction ratio without temperature control. VCSEL_1 emits at a 1550.87 nm center wavelength for downstream and VCSEL_2 emits at a 1548.27 nm center wavelength for upstream. As for the unidirectional case described above, driving voltage is 1 V peak-peak, and bias current of the VCSELs is set to 13.6 mA.

The two VCSELs are connected to opposite ends of a 40 km SSMF transmission span via optical circulators so that the received signal from VCSEL_1 can be received at the side of VCSEL_2 and vice versa while the two signals are counter-propagating in the fiber. Launch power into the fiber is 0.6 dBm in both directions.

The measured BER of the coherently detected signals before (B2B) and after bidirectional transmission over 40 km SSMF is plotted in Fig. 9 together with the measured BER after direct detection of VCSEL_1 with no counter propagating signal. B2B receiver sensitivity at the FEC limit of 2×10^{-3} for the coherent detection case is -37.7 dBm for VCSEL_1 and -39.3 dBm VCSEL_2. After 40 km transmission with the counter propagating signal, the receiver sensitivity is -37.3 and -37.7 dB for VCSEL_1 and VCSEL_2 corresponding to transmission penalties of 0.4 and 1.6 dB respectively. In order to benchmark these results against conventional direct detection unidirectional systems, the direct detection BER of VCSEL_1 after photodetection with a p-i-n type photodetector with a 3 dB bandwidth of 7.5 GHz is also plotted in Fig. 9. The receiver sensitivities for VCSEL_1 employing direct detection are –23.6 dBm B2B and –19.8 dBm after transmission, corresponding to a transmission penalty of 3.8 dB. The increased transmission penalty using direct detection is due to CD, which for the coherent detection case was compensated by DSP. Numerical simulations using *VPI Transmission Maker* yielded direct detection receiver sensitivities of –22.1 dBm B2B and –18.7 dBm after 40 km transmission, thus confirming the 3 to 4 dB transmission penalty and showing less than 1.5 dB deviation from the experiments. In the simulation, extinction ratio and chirp (alpha-parameter) were matched to the experimental eye diagram and spectrum. The low transmission penalty of the coherently detected signals shows that the CD has been successfully compensated in the DSP. The improvement in receiver sensitivity due to coherent detection for VCSEL_1 is 13.1 dB B2B and 17.5 dB after 40 km SSMF.

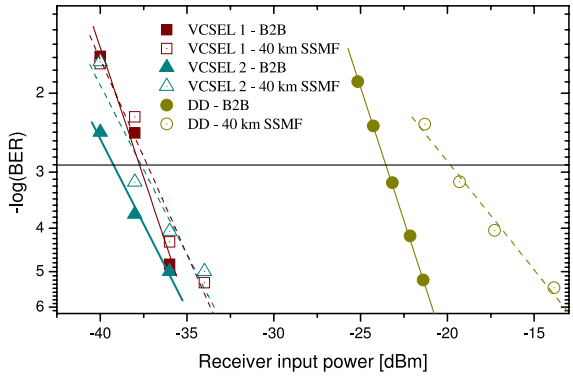

Fig. 9. BER of the bidirectional 5 Gbps coherent VCSEL demonstrations. The measured BER of a directly detected signal from a 5 Gbps modulated VCSEL is also plotted.

B. Dispersion Tolerance and Compensation

An advantage of coherent detection is the opportunity of employing DSP technique to compensate dispersion, which is particularly relevant for optical transmission in the C-band around 1550 nm wavelength where the dispersion of SSMF is approximately $17 \frac{\text{ps}}{\text{nm} \cdot \text{km}}$. In Fig. 10, the dispersion tolerance of the 1550 nm VCSEL transmission system with coherent detection has been plotted for bit rates 5 and 10 Gbps. The dispersion tolerance is estimated by applying the DSP based dispersion compensation algorithm described in Section III-A in the range -500 to $+1500$ ps/nm to the B2B signals.

As would be expected, the dispersion tolerance at 5 Gbps is much higher than at 10 Gbps. For both 5 and 10 Gbps, the optimum dispersion value is shifted from zero. This is due to

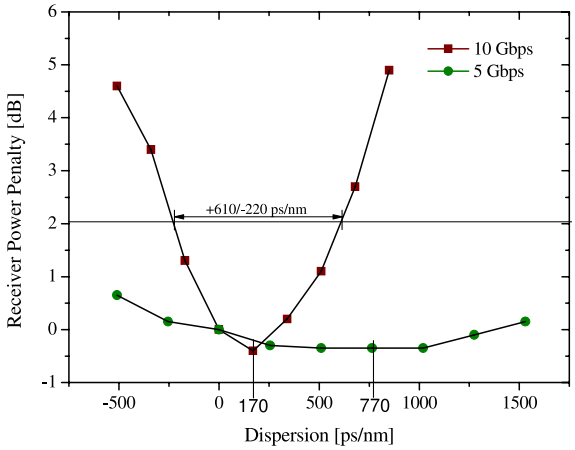

Fig. 10. Dispersion tolerance of the 1550 nm coherent VCSEL system operated at 5 and 10 Gbps.

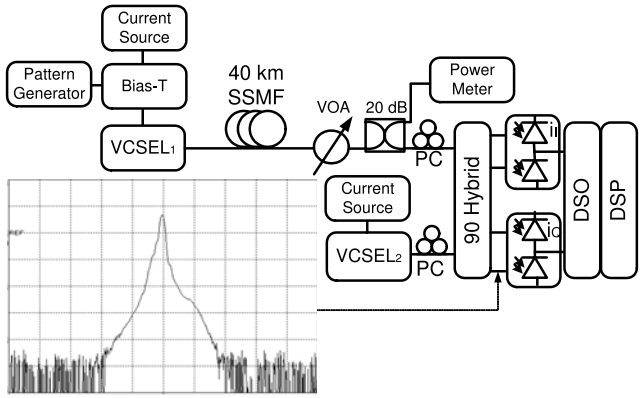

Fig. 11. Block diagram of the all-VCSEL coherent receiver implementation used in the 5 Gbps, 1550 nm transmission experiment. SSMF is standard single mode fiber, VOA is a variable optical attenuator, DSO is a digital storage oscilloscope, and DSP is digital signal processing.

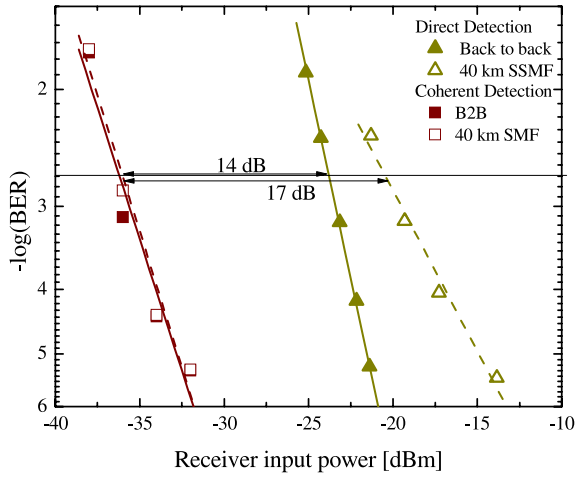

Fig. 12. BER of the 5 Gbps, 1550 nm all-VCSEL coherent experiment B2B and after 40 km SSMF transmission. BER curve of the same signal using direct detection is included for comparison.

the interplay between frequency chirp of the DM-VCSEL and CD. Optimum dispersion values are 170 ps/nm at 10 Gbps and 770 ps/nm at 5 Gbps. We also observe that the rate at which the dispersion tolerance decreases with bit rate differs from the square law relation known from chirp free on–off keying (OOK) modulation. This is due to the different relative impact of the transient and adiabatic part of the chirp from (2). Due to the longer bit period at 5 Gbps, the adiabatic part of the chirp is more dominant. The 2-dB penalty dispersion limit at 10 Gbps is -220 to $+610$ ps/nm. At 5 Gbps, the dispersion penalty is less than 1 dB in the entire range from -500 to $+1500$ ps/nm, corresponding to more than 80 km transmission. Comparing to the direct detection BER plot in Fig. 6, we see that for direct detection, there is a 3 dB dispersion induced penalty already after 40 km. It thus appears that the dispersion tolerance is higher for coherent detection than for direct detection. The reason for this is the filtering induced by the unmodulated LO laser. As the chirp separates the optical wavelength from the ones and the zeros, tuning the LO wavelength close to the ones will in effect filter out the wavelength of the zeros, thereby simultaneously improving signal extinction ratio and narrowing the optical spectrum.

C. Coherent Detection With DM-VCSEL Transmitter and VCSEL Local Oscillator

In optical access and fiber to the home systems, reducing cost is of the utmost importance. Therefore, even though it might be possible to absorb the cost of an ECL in the CO if it is shared among a high number of users, for the downstream transmission, the receiver needs to implemented in a more cost effective manner. In order to investigate this possibility, a series of experiments has been conducted, where a VCSEL was used for the LO as well as for the signal.

1) C-Band Transmission With VCSEL LO: Employing a VCSEL as the LO in VCSEL based coherent optical access systems would eliminate the main argument against coherent PONs. Due to the envelope detection based receiver implementation suggested and demonstrated in this paper, this is indeed possible. An experimental demonstration of this idea has thus been carried out. A 5 Gbps signal from a DM 1550 nm VCSEL is transmitted over 40 km SSMF, and detected with a coherent receiver using a 1550 nm VCSEL as LO. A block diagram of the setup used in the experiment is illustrated in Fig. 11. A 5 Gbps NRZ–OOK signal is combined with a dc bias current and used to directly modulate VCSEL_1. The optical signal is transmitted over a 40 km SSMF, and received by a coherent receiver consisting of an optical 90° hybrid coupler, a VCSEL LO (VCSEL_2) and two pairs of balanced photodetectors. The electrical outputs (i and q) from the photodetectors are sampled by a DSO at 40 GSa/s for off-line demodulation. The DSP demodulation algorithm is identical to the one used in the experiments employing an ECL as LO laser, and consists of dispersion compensation, envelope detection and BER calculation. The wavelength of VCSEL_2 is adjusted by tuning the bias current, and is set to be close to the wavelength of the logical '1'-state of the incoming optical signal. The combined optical spectrum of the signal and LO is shown as an insert in Fig. 11.

The BER of the 5 Gb/s signal is shown in Fig. 12. Receiver sensitivity at a BER of 2×10^{-3} is –36.5 dBm B2B as well

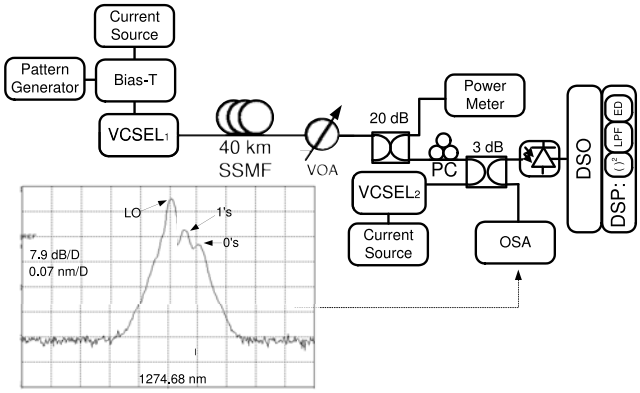

Fig. 13. Block diagram of the setup used in the O-band all-VCSEL coherent detection transmission experiments employing DSP and a simplified front-end with a 3 dB coupler instead of a 90° hybrid. SSMF is standard single mode fiber, VOA is a variable optical attenuator, DSO is a digital storage oscilloscope, and DSP is digital signal processing.

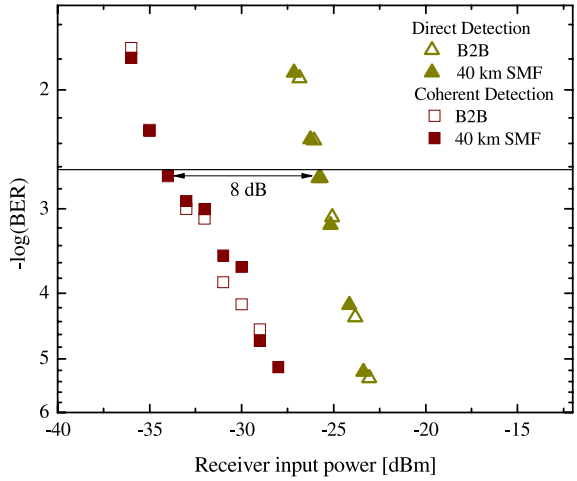

Fig. 14. BER of the 5 Gbps, 1274 nm signal back to back (B2B) and after 40 km SSMF transmission. BER curve of the same signal using direct detection is included for comparison.

as after 40 km SSMF transmission. No transmission penalty is observed. In comparison, using direct detection, receiver sensitivities of –22.5 dBm B2B and –19.5 dBm after transmission is measured as described in the previous section. Coherent detection is thus seen to provide a 14 and 17 dB improvement in receiver sensitivity B2B and after transmission respectively.

This significant improvement in receiver sensitivity for coherent detection over direct detection even when employing a VCSEL as LO underpins the capabilities of the envelope detection chirp enabled coherent detection scheme.

2) O-Band Transmission With Simplified Coherent Receiver: In order to reduce system cost by further reducing the complexity of the coherent receiver, a transmission experiment has been performed where the optical 90° hybrid has been replaced by a 3 dB coupler, and the two pairs of balanced photodiodes has been replaced by a single photodetector. As this removes the possibility of accessing both the in-phase and quadrature components of the received optical signal, digital dispersion compensation is not possible. Therefore, an O-band VCSEL emitting at 1274 nm is employed in this experiment in order to take advantage of the zero-dispersion wavelength band of SSMF. This has the advantage of further simplifying the DSP. The setup on this experiment is shown in Fig. 13.

The 1274 nm VCSEL is DM at 5 Gbps. The signal is transmitted over 40 km of SSMF, mixed with the output from a second VCSEL in a 3 dB fiber coupler, and detected by a single-ended photodetector. The combined optical spectrum of signal and LO is shown in the inset in Fig. 13. The chirp induced separation between zero-level wavelength and one-level wavelength is seen in the plot. The LO wavelength is tuned approximately 4.5 GHz offset from the one-level wavelength by adjustment of the bias current.

The BER B2B and after transmission is plotted in Fig. 14. Results for direct detection as well as coherent detection are shown. The advantage of the O-band transmission is seen in both cases, as there is no transmission penalty for neither direct detection nor for coherent detection. Receiver sensitivities are –25.7 and –33.7 dBm for direct and coherent detection respectively. The coherent detection thus gives an 8 dB improvement over direct detection.

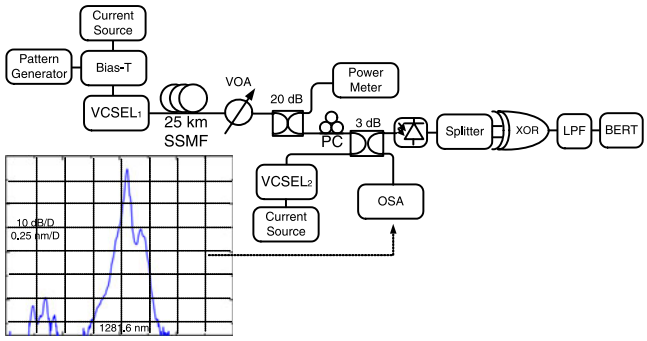

Fig. 15. Block diagram of the setup used in the real-time coherent VCSEL experiment. SSMF is standard single mode fiber, VOA is a variable optical attenuator, OSA is an optical spectrum analyzer, XOR is an electronic exclusive-or gate used as a nonlinear threshold device, LPF is a low-pass filter and BERT is a bit error rate tester.

3) O-Band Transmission With Analogue (Real-Time) Coherent Receiver: The results shown above demonstrate the possibility of reducing the complexity of a coherent receiver. Demodulation, however, is still performed with the aid of DSP. As high speed electronics becomes more and more available at ever decreasing cost, this may be realistic in just a few years. On the other hand, at present the cost of a DSP based coherent receiver for PONs would most likely be too high for the end user to accept. Therefore an analog receiver implementation without DSP represents an attractive stepping stone on this path. As the DSP used in the receiver is really not much more than envelope detection followed by low pass filtering, an analog implementation is indeed possible. In addition, such an implementation would show that the DSP based results presented here can be realized real time.

In Fig. 15, the setup used in the experimental demonstration of one possible analog implementation is shown. Signal generation, transmission and the optical front end of the receiver is identical to the DSP based simplified receiver setup shown in

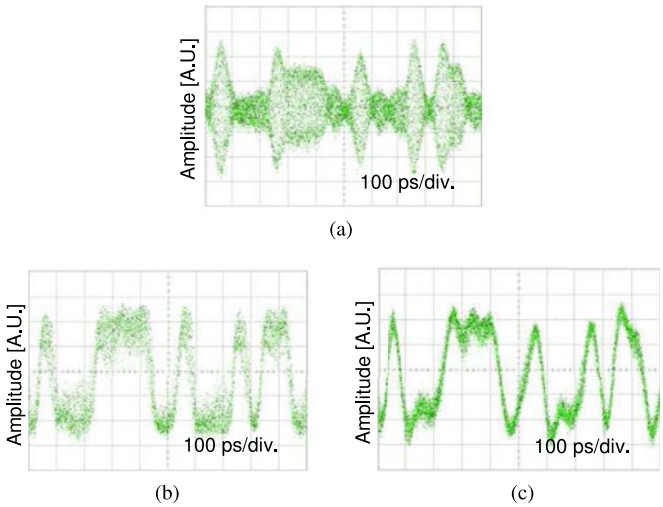

Fig. 16. (a) The coherently detected signal after the photodetector, (b) after inverted self-XOR gating and (c) after additional low pass filtering. (a) After photodetector. (b) After XOR gate. (c) After LPF.

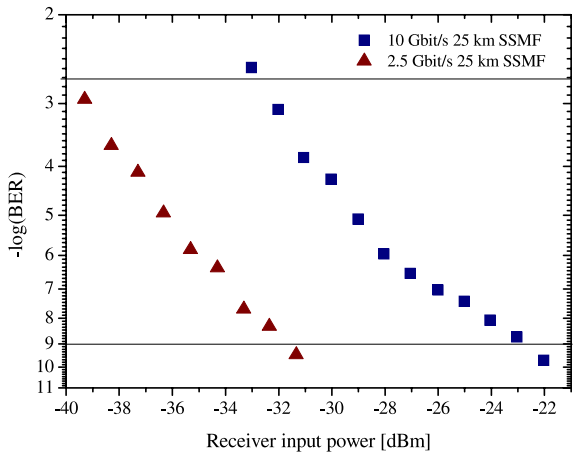

Fig. 17. BER back to back (B2B) and after transmission of the 2.5 and 10 Gbps O-band all-VCSEL real-time coherent detection experiment.

Fig. 13 apart from an upgrade in bit rate from 5 to 10 Gbps. In addition, the performance at 2.5 Gbps is tested. The signal after photodetection is shown in Fig. 16(a). The RF-like nature of the signal is evident, with a low signal level in the zeros and a high level fluctuating signal in the ones. After photodetection, in stead of a DSO, the envelope detection is performed by an electronic gate with a nonlinear threshold followed by a low-pass filter. In our demonstration, an exclusive-or gate (XOR) performs the task of nonlinear thresholding by biasing it below threshold, and feeding the same signal (from a 6 dB power splitter) to the two inputs. The signal after the nonlinear thresholding in the XOR gate is shown if Fig. 16(b). Low pass filtering, shown in Fig. 16(c), removes high frequency ripples, and the original NRZ signal is restored and evaluated by a bit error rate tester.

The BER of the O-band 2.5 and 10 Gbps signals after transmission employing analog real-time coherent receiver is plotted in Fig. 17. Receiver sensitivity is –32.5 dBm at 10 Gbps and –40 dBm at 2.5 Gbps. Numerical simulations using *VPI transmission maker* estimates the direct detection receiver sensitivities at 1274 nm wavelength to be –22 dBm at 10 Gbps and –22.7 dBm at 2.5 Gbps. The estimated improvement in receiver sensitivity achieved by employing the proposed real time analog coherent receiver implementation in stead of conventional direct detection is thus 10.5 dB at 10 Gbps and 17.3 dB at 2.5 Gbps.

TABLE I
SUMMARY OF RECEIVER SENSITIVITY AT A BER OF 2×10^{-3} AND PASSIVE SPLIT RATIO ASSUMING 40 km SSMF TRANSMISSION AND 0.6 dBm LAUNCH POWER

	Rec. Sens. [dB]	Split ratio
5 Gbps C-band ECL LO	–37.3	1024
5 Gbps C-band VCSEL LO	–36.5	512
10 Gbps C-band ECL LO	–34	512
2.5 Gbps O-band VCSEL LO	–40	512
5 Gbps O-band VCSEL LO	–33.7	128
10 Gbps O-band VCSEL LO	–32.5	64

D. Summary of Results

The previously described experimental demonstrations of various flavors of VCSEL based coherent PONs all illustrate the potential offered by this technology. In order to quantify this potential, the power budget and passive split ratio has been collected in Table I assuming 40 km transmission, and fiber attenuation of 0.2 dB/km in the C-band and 0.35 dB/km in the O-band. Note that these numbers represent ideal values where, e.g., fiber aging, splice loss and excess loss in power splitters are not considered.

If the all-VCSEL coherent detection techniques are to be used in a WDM–PON system, 3 dB should be allocated for loss in the AWG used to combine the signals in the CO. This would result in 3 dB lower power budget margin and hence half the allocated splitting ratio compared to what is listed in the table.

IV. CONCLUSION

The requirements imposed on next generations of optical access networks by the EU in their digital agenda for 2020 and by FSAN in their target specifications for NG-PON2 presents a dilemma for the FTTx providers. On one hand, conventional TDM–PON is unable to meet the demands, and on the other hand, optical amplifiers, AWG based WDM, and/coherent detection as implemented in the core networks is to complex and costly to deploy in optical access.

This paper reviews investigations of the possibility of meeting the NG-PON2 requirements without sacrificing simplicity through the employment of a simplified coherent detection scheme based on coherent detection of signals from DM-VCSELs.

In a series of experiments, it has been demonstrated that it is indeed possible to employ DM-VCSELs as transmitters in coherent PON which even employ VCSELs as LOs. The proposed envelope detection scheme has been demonstrated in a digital implementation using off-line processing and in an analogue implementation where the nonlinear transfer function of an XOR gate has been utilized. Experiments have been carried out in the C-band around 1550 nm as well as in the O-band around 1300 nm. Receiver sensitivities better than –37.3 dBm

at 5 Gbps suggests a potential 1024-times passive splitting ratio after 40 km SSMF transmission in the C-band. Due to the higher fiber attenuation in the O-band, splitting ratio at 5 Gbps is limited to 128 times if the 40 km reach is maintained. Reducing the bit rate to 2.5 Gbps, however, brings the achievable splitting ratio up to 512.

The chirp enabled envelope detector eliminates the need for phase tracking, and therefore shows a path towards coherent detection using low-cost lasers. In these experiments, a manually operated polarization controller is used to align the polarization of the LO with that of the signal. Automatic polarization control, e.g., by monitoring the power after LO/signal beating, or a polarization diversity receiver should be implemented in a commercial system. This will add to the cost and complexity of the system, and should therefore be carefully weighed against the advantages of coherent detection.

These results show that coherent PONs solely based on VCSELs is a very strong candidate for NG-PON2, capable of meeting demands from the FSAN and the EU while maintaining the simplicity required for optical access networks. Future work will include WDM demonstrations with receiver side channel selection by LO tuning and real-time digital demodulation in a field programmable gate array.

ACKNOWLEDGMENT

The authors would like to thank Vertilas for providing the C-band VCSELs, Alight Technologies for providing the O-band VCSELs and Aragon Photonics for the loan of the BOSA Phase Optical Complex Spectrum Analyzer. We would also like to thank Dr. T. B. Gibbon for performing the BOSA Phase measurements.

REFERENCES

[1] Digital agenda 2020—Pillar IV: Fast and ultra-fast Internet access. [Online]. Available: https://ec.europa.eu/digital-agenda/en/our-goals/pillar-iv-fast-and-ultra-fast-internet-access

[2] The full service access networks (FSAN) group. [Online]. Available: https://FSAN.org

[3] R. Rodes, J. B. Jensen, D. Zibar, C. Neumeyr, E. Roenneberg, J. Rosskopf, M. Ortsiefer, and I. T. Monroy, "All-VCSEL based digital coherent detection link for multi Gbit/s WDM passive optical networks," *Opt. Exp.*, vol. 18, no. 24, pp. 24969–24974, 2010.

[4] J. B. Jensen, R. Rodes, D. Zibar, and I. T. Monroy, "Coherent detection for 1550-nm, 5-Gbit/s VCSEL-based 40-km bidirectional PON transmission," in *Proc. Conf. Opt. Fiber Commun., Collocated Nat. Fiber Opt. Eng. Conf.*, 2011.

[5] R. Rodes, J. B. Jensen, A. Caballero, and I. T. Monroy, "1.3 μm all-VCSEL low complexity coherent detection scheme for high bit rate and high splitting ratio PONs," in *Proc. Conf. Opt. Fiber Commun., Collocated Nat. Fiber Opt. Eng. Conf.*, 2011, p. 5875438.

[6] R. Rodes Lopez, N. Cheng, J. B. Jensen, and I. Tafur Monroy, "10-Gb/s real-time All-VCSEL low complexity coherent scheme for PONs," in *Proc. Conf. Opt. Fiber Commun., Collocated Nat. Fiber Opt. Eng. Conf.*, 2012, p. 6191986.

[7] S. Wilson. (2012). The race for NGPON 2 heats up as two contenders stand out. [Online]. Available: *Informa telecoms and media—http://blogs.informatandm.com/4120/the-race-for-ngpon-2-heats-up-as-two-contenders-stand-out/*

[8] H. Rohde, S. Smolorz, J. S. Wey, and E. Gottwald, "Coherent optical access networks," in *Proc. Conf. Opt. Fiber Commun., Collocated Nat. Fiber Opt. Eng. Conf.*, 2011, p. 5875538.

[9] G. de Valicourt, M. Lamponi, G. H. Duan, F. Poingt, M. Faugeron, P. Chanclou, and R. Brenot, "First 100-km uplink transmission at 2.5 Gbit/s for hybrid WDM/TDM PON based on optimized bi-electrode RSOA," in *Proc. 36th Eur. Conf. Exhibit. Opt. Commun.*, 2010, p. 5621160.

[10] K. Y. Cho, U. H. Hong, Y. Takushima, A. Agata, T. Sano, M. Suzuki, and Y. C. Chung, "103-Gb/s long-reach WDM PON implemented by using directly modulated RSOAs," *IEEE Photon. Technol. Lett.*, vol. 24, no. 3, pp. 209–211, Feb. 2012.

[11] H. Zhang, X. Cheng, Z. Xu, and Y.-K. Yeo, "A novel combined WDM–PON with a single shared DI using downlink DPSK and uplink remodulated OOK signals," *Opt. Commun.*, vol. 285, no. 6, pp. 992–996, 2012.

[12] L. Yi, Z. Li, T. Zhang, Y. Dong, W. Hu, and D. Lin, "10-Gb/s symmetric WDM–PON using stable multi-longitudinal mode Brillouin/SOA fiber laser as upstream colorless source," *Chinese Opt. Lett.*, vol. 9, no. 12, p. 120603, 2011.

[13] L. Liu, M. Zhang, M. Liu, X. Zhang, and P. Ye, "Design and analysis of flexible colorless remote node using RSOA-assisted Michelson interferometer," *Chin. Opt. Lett.*, vol. 9, no. 2, pp. 20606–20609, 2011.

[14] J. B. Jensen, I. T. Monroy, R. Kjaer, and P. Jeppesen, "Reflective SOA remodulated 20 Gbit/s RZ-DQPSK over distributed Raman amplified 80 km long reach PON link," *Opt. Exp.*, vol. 15, no. 9, pp. 5376–5381, 2007.

[15] D. Shin, D. Jung, H. Shin, J. Kwon, S. Hwang, Y. Oh, and C. Shim, "Hybrid WDM/TDM-PON for 128 subscribers using λ-selection-free transmitters," *OSA Trends Opt. Photon. Series*, vol. 95B, pp. 652–654, 2004.

[16] F.-T. An, K. S. Kim, Gutierrez, Yam, Hu, Shrikhande, and Kazovsky, "SUCCESS: A next-generation hybrid WDM/TDM optical access network architecture," *IEEE J. Lightw. Technol.*, vol. 22, no. 11, pp. 2557–2569, Nov. 2004.

[17] J. Segarra, C. Bock, and J. Prat, "Hybrid WDM/TDM PON based on bidirectional reflective ONUs offering differentiated QoS via OBS," in *Proc. 7th Int. Conf. Transp. Opt. Netw.*, 2005, vol. 1, pp. 95–100.

[18] F. Payoux, P. Chanclou, T. Soret, N. Genay, and R. Brenot, "Demonstration of a RSOA-based wavelength remodulation scheme in 1.25 Gbit/s bidirectional hybrid WDM–TDM PON," in *Proc. Conf. Opt. Fiber Commun., Collocated Nat. Fiber Opt. Eng. Conf.*, 2006, pp. 46–48.

[19] L. Kazovsky, N. Cheng, W.-T. Shaw, and S.-W. Wong, "CROWN—converged optical and wireless networks: Network architecture and routing algorithms," in *Proc. 9th Int. Conf. Transp. Opt. Netw.*, 2007, vol. 1, pp. 266–269.

[20] Y.-B. Choi and S.-J. Park, "The low cost hybrid CWDM/DWDM-TDM-PON system for next FTTH," in *Proc. Asia Opt. Fiber Commun. Optoelectron. Expo. Conf.*, 2008, p. 5348730.

[21] J. Chen, L. Wosinska, and S. He, "High utilization of wavelengths and simple interconnection between users in a protection scheme for passive optical networks," *IEEE Photon. Technol. Lett.*, vol. 20, no. 5–8, pp. 389–391, Mar. 2008.

[22] M. M. De Laat, R. L. Duijn, E. G. C. Pluk, G. N. Van Den Hoven, P. J. Urban, and H. De Waardt, "FlexPON: A hybrid TDM/WDM network enabling dynamic bandwidth reconfiguration using wavelength routing," in *Proc. 35th Eur. Conf. Opt. Commun.*, 2009, p. 5288427.

[23] P. Ossieur, C. Antony, A. M. Clarke, A. Naughton, H.-G. Krimmel, Y. Chang, C. Ford, A. Borghesani, D. G. Moodie, A. Poustie, R. Wyatt, B. Harmon, I. Lealman, G. Maxwell, D. Rogers, D. W. Smith, D. Nesset, R. P. Davey, and P. D. Townsend, "A 135-km 8192-split carrier distributed DWDM–TDMA PON with $2 \times 32 \times 10$ Gb/s capacity," *IEEE J. Lightw. Technol.*, vol. 29, no. 4, pp. 463–474, Feb. 2011.

[24] Z. Li, L. Yi, Y. Zhang, Y. Dong, S. Xiao, and W. Hu, "Compatible TDM/WDM PON using a single tunable optical filter for both downstream wavelength selection and upstream wavelength generation," *IEEE Photon. Technol. Lett.*, vol. 24, no. 10, pp. 797–799, May 2012.

[25] G. Das, B. Lannoo, A. Dixit, D. Colle, M. Pickavet, and P. Demeester, "Flexible hybrid WDM/TDM PON architectures using wavelength selective switches," *J. Opt. Switch. Network.*, vol. 9, no. 2, pp. 156–169, 2012.

[26] B. Glance, O Scaramucci, T. L. Koch, K. C. Reichmann, L. D. Tzeng, U. Koren, and G. A. Burrus, "Densely spaced FDM coherent optical system with random access digitally tuned receiver," in *Proc. IEEE Global Telecommun. Conf. Exhib.*, 1989, pp. 343–345.

[27] G. D. Marchis, M. Listani, F. M. Fondazione, and U. Bordoni, "Polarization modulation in multi-wavelength passive optical networks," in *Proc. Eur. Fibre Opt. Commun. Local Area Netw. Conf.*, 1990, pp. 26–30.

[28] V. C. M. Leung and F. Takawira, "FDM packet multiple access network using coherent fibre optic communication," vol. 4, pp. 1648–1652, 1990.

[29] Q. Jiang and M. Kavehrad, "An optical multiaccess star network using subcarrier multiplexing," *IEEE Photon. Technol. Lett.*, vol. 4, no. 10, pp. 1163–1165, Oct. 1992.

[30] A. A. de Albuquerque, "High speed optical networks projects in the EC RACE programme: From the customer access connection to the transit

network," in *Proc. IEEE Int. Conf. Commun.*, 1993, vol. 2, pp. 1215–1219.

[31] E.-J. Bachus, T. Almeida, P. Demeester, G. Depovere, A. Ebberg, M. R. Ferreira, G.-D. Khoe, O. Koning, O. Marsden, R. Rawsthorne, and N. Wauters, "Coherent optical systems implemented for business traffic routing and access: The RACE COBRA project," *IEEE J. Lightwave Technol.*, vol. 14, no. 6, pp. 1309–1319, Jun. 1996.

[32] C. Brisson, A. Kung, P. Nicati, P. Robert, D. Rodellar, and C. Bungarzeanu, "New multichannel optical local area network based on an original star topology with an adapted multi-Ethernet protocol," in *Proc. SPIE— Int. Soc. Opt. Eng.*, 1998, vol. 3491, pp. 495–500.

[33] S. Narikawa, N. Sakurai, K. Kumozaki, and T. Imai, "Coherent WDM–PON based on heterodyne detection with digital signal processing for simple ONU structure," in *Proc. Eur. Conf. Opt. Commun. Proc.*, 2006, p. 4801085.

[34] J. M. Fabrega and J. Prat, "Ultra-dense, transparent and resilient ring-tree access network using coupler-based remote nodes and homodyne transceivers," in *Proc.11th Int. Conf. Transp. Opt. Netw.*, 2009, pp. 450–453.

[35] N. Cvijetic, D. Qian, J. Hu, and T. Wang, "44-Gb/s/λ, upstream OFDMA–PON transmission with polarization-insensitive source-free ONUs," in *Proc. Conf. Opt. Fiber Commun., Collocated Nat. Fiber Opt. Eng. Conf.*, 2010, p. 5465177.

[36] Z. Dong, J. Yu, H.-C. Chien, Z. Dong, L. Chen, J. Yu, N. Chi, Z. Dong, and G.-K. Chang, "Ultra-dense WDM–PON delivering carrier-centralized Nyquist-WDM uplink with digital coherent detection," *Opt. Exp.*, vol. 19, no. 12, pp. 11100–11105, 2011.

[37] D. Fritzsche, E. Weis, and D. Breuer, "Potential of OFDM for next generation optical access," in *Proc. SPIE— Int. Soc. Opt. Eng.*, 2011, vol. 7959, no. 1, pp. 795905–795906.

[38] A. V. Osadchiy, K. Prince, N. G. Gonzalez, A. Caballero, F. O. Amaya, J. B. Jensen, D. Zibar, and I. T. Monroy, "Coherent detection passive optical access network enabling converged delivery of broadcast and dedicated broadband services," *Opt. Fiber Technol.*, vol. 17, no. 1, pp. 1–6, 2011.

[39] N. G. Gonzalez, A. C. Jambrina, R. Borkowski, V. Arlunno, T. T. Pham, R. Rodes, X. Zhang, M. B. Othman, K. Prince, X. Yu, J. B. Jensen, D. Zibar, and I. T. Monroy, "Reconfigurable digital coherent receiver for metro-access networks supporting mixed modulation formats and bit-rates," in *Proc. Conf. Opt. Fiber Commun., Collocated Nat. Fiber Opt. Eng. Conf.*, 2011, p. 5875364.

[40] M. Zhu, J. Liu, Y.-T. Hsueh, G.-K. Chang, J. Liu, G. Gu, and F. Zhu, "Terabit optical access networks using ultra-dense WDM and coherent technology," in *Proc. SPIE—Int. Soc. Opt. Eng.*, 2012, vol. 8331, p. 83310G.

[41] N. Cvijetic, M.-F. Huang, E. Ip, Y. Shao, Y.-K. Huang, M. Cvijetic, and T. Wang, "Coherent 40 Gb/s OFDMA–PON for long-reach (100+km) high-split ratio (1:64) optical access/metro networks," in *Proc. Conf. Opt. Fiber Commun., Collocated Nat. Fiber Opt. Eng. Conf.*, 2012, p. 6192193.

[42] R. Gaudino, V. Curri, G. Bosco, G. Rizzelli, A. Nespola, D. Zeolla, S. Straullu, S. Capriata, and P. Solina, "On the use of DFB lasers for coherent PON," in *Proc. Conf. Opt. Fiber Commun., Collocated Nat. Fiber Opt. Eng. Conf.*, 2012, p. 6191985.

[43] J. Prat, V. Polo, I. Cano, J. Tabares, P. Zakynthinos, D. Klonidis, J. M. Fabrega, and I. Tomkos, "Simple intradyne PSK system for UDWDM–PON," *Opt. Exp.*, vol. 20, no. 27, pp. 28758–28763, 2012.

[44] N. Yoshimoto, J. Kani, S.-Y. Kim, N. Iiyama, and J. Terada, "DSP-based optical access approaches for enhancing NG–PON2 systems," *IEEE Commun. Mag.*, vol. 51, no. 3, pp. 58–64, Mar. 2013.

[45] (2012). FSAN close to choosing the next generation of PON. [Online]. Available: http://www.gazettabyte.com/, vol. 4, no. 4.

[46] S.-Y. Kim, N. Sakurai, H. Kimura, and H. Hadama, "VCSEL-based coherent detection of 10-Gbit/s QPSK signals using digital phase noise cancellation for future optical access systems," in *Proc. Conf. Opt. Fiber Commun., Collocated Nat. Fiber Opt. Eng. Conf.*, 2010, p. 5465283.

[47] C. Xie, P. Dong, P. Winzer, C. Gréus, M. Ortsiefer, C. Neumeyr, S. Spiga, and M Müller, M.-C. Amann, "960-km SSMF transmission of 105.7-Gb/s PDM 3-PAM using directly modulated VCSELs and coherent detection," *Opt. Exp.*, vol. 21, no. 9, pp. 11585–11589, 2013.

[48] G. P. Agrawal, *Fiber-Optic Communication Systems*, 3rd ed. New York, NY, USA: Wiley-Interscience, 2002.

[49] T. L. Koch and R. A. Linke, "Effect of nonlinear gain reduction on semiconductor laser wavelength chirping," *Appl. Phys. Lett.*, vol. 48, no. 10, pp. 613–615, 1986.

[50] C. Harder, K. Vahala, and A. Yariv, "Measurement of the linewidth enhancement factor alpha of semiconductor-lasers," *Appl. Phys. Lett.*, vol. 42, no. 4, pp. 328–330, 1983.

[51] C. Henry, "Theory of the linewidth of semiconductor-lasers," *IEEE J. Quantum Electron.*, vol. 18, no. 2, pp. 259–264, Feb. 1982.

[52] T. Gibbon, K. Prince, T. Pham, A. Tatarczak, C. Neumeyr, E. Rönneberg, M. Ortsiefer, and I. T. Monroy, "VCSEL transmission at 10 Gb/s for 20-km single-mode fiber WDM–PON without dispersion compensation or injection locking," *Opt. Fiber Technol.*, vol. 17, no. 1, pp. 41–45, 2011.

Authors' biographies not available at the time of publication.